Biophysical Chemistry, 38 (1990) 201–211
Elsevier

BIOCHE 01456

Conformation of intercalated DNA plasmids investigated by circular dichroism and dynamic light scattering

G. Chirico, L. Lunelli and G. Baldini

Dipartimento di Fisica, Università di Milano, Via Celoria 16, 20133 Milano, Italy

Received 23 October 1989
Revised manuscript received 7 March 1990
Accepted 13 March 1990

Circular dichroism; Dynamic light scattering; Plasmid; DNA; Conformation; Ethidium bromide

Two DNA plasmids, pEGF and pACL29, intercalated with ethidium bromide (EB), have been examined by circular dichroism (CD) and dynamic light scattering (DLS). CD and DLS data show significant changes when the EB/DNA (phosphates) ratio reaches a value of $r \cong 0.13$. The translational and rotational diffusion coefficients, predicted assuming that plasmids can be described by a string of beads, and the CD spectrum, suggest that a transition from an interwound to a toroidal conformation is likely to occur.

1. Introduction

The role of DNA secondary and tertiary structures has long been assumed in the expression of its biological activity. In particular, the achievement of the superhelical conformation appears to act as a switch of biological activity [1].

In the past, the study of the secondary structure of DNA has been performed mainly with X-ray diffraction on DNA fibers, and some results have also been obtained from circular dichroism (CD) on both DNA fibers and solutions. The geometrical parameters of the DNA helix [2] in crystals or fibers seem to be fairly well established. While the X-ray technique has provided detailed information on the atomic positions, CD spectra have yielded good 'fingerprints' of the different DNA forms. Several works have contributed to the assignment of characteristic CD spectra to different DNA helix forms (A, B, ...Z) [3,4].

CD has proved to be very sensitive to changes in the secondary structure of DNA, however, its sensitivity to the tertiary structure has been less extensively investigated. The majority of studies of the conformation of DNA have been devoted to DNA-histone structure [5]. In principle, CD should not be very sensitive to the overall structure of DNA, since it depends mainly on the interaction (dipole-dipole) between chromophores which are only a few tens of ångstroms apart. Therefore, any dependence of CD on the tertiary structure of DNA appears to be linked to a change in the secondary structure as well [6].

Whilst the secondary structure is well established, at least in fibers and crystals, knowledge of the tertiary structure is lacking in depth. The secondary structure of DNA fibers is usually considered to be reasonably similar to that of DNA in solution. However, the configuration of DNA in fibers and crystals probably bears little resemblance to that in solution owing to the extremely different interactions of the molecule with the surrounding medium. In fact, the interactions of DNA with solvent and other molecules have long been recognized as fundamental in determining

Correspondence address: G. Baldini, Dipartimento di Fisica, Università di Milano, Via Celoria 16, 20133 Milano, Italy.

0301-4622/90/$03.50 © 1990 Elsevier Science Publishers B.V. (Biomedical Division)

both the secondary and tertiary structure, and in the regulation of DNA biological activity [1]. The present article is aimed at the elucidation of links between the secondary and tertiary structure of DNA in solutions.

In order to pursue this goal, plasmid DNAs, which are covalently closed circular molecules with known base-pair sequences, have been investigated. It should be noted that plasmids exhibit an additional link between secondary and tertiary structure as a result of the closure conditions for a circular DNA. Finally, the study of plasmid DNA may be relevant as regards a number of biological aspects, since chromosomal DNA forms small domains with two ends fixed to the chromosome core and the domain's topological properties are identical to those of plasmid DNAs [1,7].

Here, two different DNA plasmids, either in the native form or nicked, have been studied by using CD and dynamic light scattering (DLS) experiments in the presence of ethidium, an intercalator that can alter the structure of DNA. CD, which is particularly suited to the study of conformational changes and local structure, can lead to useful information about the secondary structure (local ordering). DLS, which is based on the measurement of the time correlation function of the light scattered from a molecular solution, allows the evaluation of the diffusion coefficients of a macromolecule and estimation of its slowest internal motions [8,9], thereby clarifying mainly the tertiary structure.

2. Materials and methods

The plasmids DNAs used were pACL29 (pBR322-derived) and pEGF (pUC18-derived), a plasmid with an insertion of known composition. The number of base-pairs in pACL29 and pEGF is 5400 and 3220, respectively. pEGF was a gift from F. Badaracco (Department of Biology, Milan University) and pACL29 was kindly donated by J. Langowski (EMBL, Grenoble, France). Both plasmids were replicated by harbouring in Coli HB101 as described previously [8].

After precipitation with polyethylene glycol, the purity of the crude DNA was assessed by electrophoresis on a 1% agarose gel which showed the precipitate to be almost pure (80–90%) plasmid DNA in superhelical form.

The DNA was then purified by HPLC [8], the final stage being performed using a CsCl gradient. Ethidium, used for the gradient, was removed by several steps of butanol extraction and the solution was dialysed several times vs 10 mM Tris-EDTA buffer. A second electrophoretic run showed that only a few percent of linear DNA and dimeric plasmid were present. This DNA was then precipitated with ethanol, dried under vacuum and stored at 4°C.

2.1. Nicked plasmids

Nicked plasmids were obtained by digestion with DNAase I (RNAase free, Boehringer). The concentration of DNAase used for digestion was 0.01 U/μl for 250 μg/ml DNA solutions. The samples were left for 10 min on ice for digestion and the process stopped by adding EDTA (pH 8.0) up to 30 mM. After nicking, DNA was purified by removal of proteins via phenol, chloroform and ether extractions, precipitated with ethanol, dried under vacuum and stored at 4°C. DNAs used in measurements were dissolved in phosphate buffer (10 mM KH_2PO_4, 30 mM Na_2HPO_4, 0.1 mM Na_3EDTA; pH 7.35, ionic strength 100 mM).

Concentrations were determined from absorption measurements on a Perkin-Elmer 555 spectrometer. The molar extinction coefficients employed were $\epsilon(260\ nm) = 6600\ M^{-1}\ cm^{-1}$ [10] for plasmids, and $\epsilon(480\ nm) = 5860\ M^{-1}\ cm^{-1}$ for ethidium [11]. DNA concentration is expressed in mol phosphate/l solution.

Data on the titration curves with ethidium (EB) were obtained by spectrofluorometry. These measurements were performed on a Perkin Elmer 650-40 fluorescence spectrometer. The wavelengths used for excitation λ (λ_{exc}) and emission (λ_{em}) were 500 and 608 nm, respectively.

CD measurements were recorded on a J-500A spectropolarimeter (Jasco, Japan). The instrument was checked as suggested by Davidson and Norden [12,13] and the CD spectra were found not to require any appreciable correction for the photo-

elastic cell parameters. The CD spectra were sent via an AD converter to a PC computer where data analysis was performed. Data on the ethidium-DNA complex within the range 220–350 nm were collected using a 1.0 cm long Hellma quartz cell: a 10.0 cm home-made cell was used in the region of very low ethidium concentration. The CD baseline of all cells was low compared with the usual CD signals and was subtracted from the spectra. The CD spectra are reported as the difference in molar extinction coefficient for left and right circular polarized light:

$$\Delta\epsilon = \epsilon_l - \epsilon_r \tag{1}$$

The molar extinction coefficient ϵ ($M^{-1}\,cm^{-1}$) of DNA refers to the absorbance per unit concentration of phosphate.

DLS measurements were performed using a specially built optical setup [8]. The light source was a Spectra Physics 25 mW He-Ne laser and the correlation functions were analyzed on a Malvern log-lin 7027 correlator. The intensity correlation functions $C(t)$ sampled at small angles (25–30°) yielded good fits when using only a single exponential:

$$C(t) = C(\infty)\left(1 + \left[A \cdot \exp(-t/\tau)\right]^2\right. \tag{2}$$

whereas those at larger angles required double-exponential analysis:

$$C(t) = C(\infty)\left(1 + \left[A \cdot \exp(-t/\tau_1) + B \cdot \exp(-t/\tau_2)\right]^2\right) \tag{3}$$

This is also expected on the basis of theory, since when considering examples such as a supercoiled interwound DNA approximated by a cylinder (e.g., 350 nm length × 15 nm diameter), one obtains a value of the order of 0.1% for the contribution of the second exponential ($B \cdot \exp(-t/\tau_2)$; eq.3).

The relaxation times τ_1 and τ_2 are equal to $(D_t K^2)^{-1}$ and $(D_2 K^2)^{-1}$, respectively. In these definitions, K^2 is equal to $4\pi n \cdot [\sin(\theta/2)] \cdot (1/\lambda)$, λ being the wavelength of light, n the refractive index and θ the angle between the incident and scattered beams. Further details of the instrument and data analysis can be found elsewhere [8,9].

3. CD spectra

The CD spectra were recorded for both the native and nicked forms of pEGF and pACL29 plasmids. The spectra appear B-like and the small differences between the two forms are within the limits of experimental error ($\Delta\epsilon = \pm 0.1$).

CD measurements on native DNAs and on their nicked forms in the presence of ethidium were performed. For each DNA, the ethidium (D)/DNA phosphate (P) molar concentration ratio, D/P, spans the range 0–0.14.

Using the same samples as for CD, fluorometric studies were performed in order to determine the fraction of bound ethidium. The fluorometric data were analyzed following the usual scheme [14]. The fluorescence intensity, $I_F = \eta_f C_f + \eta_b C_b$, was evaluated at various values of the D/P ratio. η_f, η_b, C_f and C_b denote the fluorescence efficiency and concentration of the free and bound ethidium molecules, respectively.

η_f is estimated from solutions of ethidium in 100 mM phosphate buffer, while η_b is obtained from measurements on DNA-ethidium solution at very low D/P ($D/P \cong 0.002$).

From such measurements, the amount of intercalating agent bound to DNA (C_b) can be estimated. We usually take the ratio $r = C_b/P$ as an indicator of the degree of intercalation.

3.1. CD spectra of DNA-ethidium complex

The CD spectra of calf thymus (CT) DNA with and without ethidium are shown in fig. 1. A band at 308 nm and changes in the short-wavelength region of the CD spectrum are the most noticeable effects of intercalation, as reported previously by Aktipis et al. [15]. In order to demonstrate the differences between the CD spectra of DNA and those of the DNA-ethidium complex, we report CD difference spectra, defined as the CD of the DNA-ethidium complex ($\Delta\epsilon_c$) minus that of DNA ($\Delta\epsilon_p$), at the same DNA concentration as in the intercalated sample (fig. 1c):

$$\Delta^*\epsilon = \Delta\epsilon_c - \Delta\epsilon_p \tag{4}$$

The CD difference spectrum of calf thymus (CT)

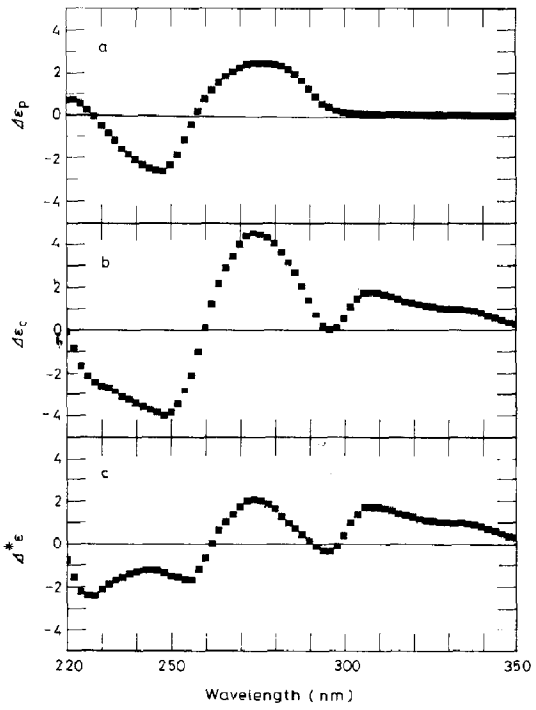

Fig. 1. (a) CD spectrum ($\Delta\epsilon_p$ (in $M^{-1}\,cm^{-1}$) of calf thymus DNA without ethidium, (b) $\Delta\epsilon_c$ ($M^{-1}\,cm^{-1}$) with ethidium at $r \cong 0.1$ and (c) difference $\Delta^*\epsilon$ ($M^{-1}\,cm^{-1}$) of the above CD spectra.

DNA shows two major positive bands, one at $\lambda \cong 308$ nm and another at $\lambda \cong 275$ nm. The difference spectra $\Delta^*\epsilon$ for the two native plasmids pEGF and pACL29 are depicted in fig. 2. From fig. 2, one observes that $\Delta^*\epsilon$ in the region 250–280 nm is significantly less than that in the case of CT-DNA.

In order to elucidate the origin of the differences between CT-DNA (linear) and plasmid (circular) DNA, CD investigation of the nicked forms of both plasmids was performed. As shown by the plots (fig. 2), the $\Delta^*\epsilon$ spectra for nicked and CT-DNA in the 250–280 nm region are comparable.

3.2. EB-induced changes in DNA structure

In order to discuss the CD difference spectra reported in figs. 1 and 2, we shall now consider some of the properties of the EB-DNA complex. It is known that after EB binding, the number of helical turns changes, due to DNA unwinding by an angle of $\delta\phi = -26°$ per EB molecule [16,17]. As a consequence of the well-known relation between linking (α) and twisting number (β):

$$\alpha = \beta + \tau \tag{5}$$

the superhelix number τ also varies [18–20]. It should be noted that α is a topological invariant parameter of the closed molecule. The change in twisting number β induced by EB binding is expressed as:

$$\delta\beta = \beta_0 \delta\phi \frac{10r}{180} \tag{6}$$

where β_0 denotes the twisting number of DNA in its native B-DNA form.

On the basis of eq. 5, τ will change by the amount $\Delta\tau = -\Delta\beta$. The law that predicts the behavior of τ vs r is therefore:

$$\tau = \tau_0 - \beta_0 \delta\phi \frac{10r}{180} \tag{7}$$

where τ_0 is the superhelical turn number of DNA in the native form ($r = 0$).

Four bands are present in the ultraviolet range (227, 254, 275 and 308 nm) and the absolute values of their maxima are plotted in fig. 3 for the two plasmids and CT DNA (solid lines). The behavior of the nicked plasmids is similar to that of linear CT DNA. In contrast, the CD difference spectra $\Delta^*\epsilon$ show different behavior when native and nicked plasmids are compared, especially in the 254 and 275 nm bands.

The behavior of the 227 nm band vs r suggests a local interaction of ethidium with neighboring bases. This band, in fact, shows linear behavior of its peak strength vs r which is almost the same among all of the different DNAs investigated. This linear behavior is indicative of a non-exciton interaction between different bound ligands [15].

The 308 nm band is almost certainly due to ethidium, since it is at a wavelength distant from that of the DNA CD spectra. The trend toward quadratic behavior of this band vs r suggests the occurrence of (i) an exciton effect [15] between neighboring dye molecules, or (ii) increasing de-

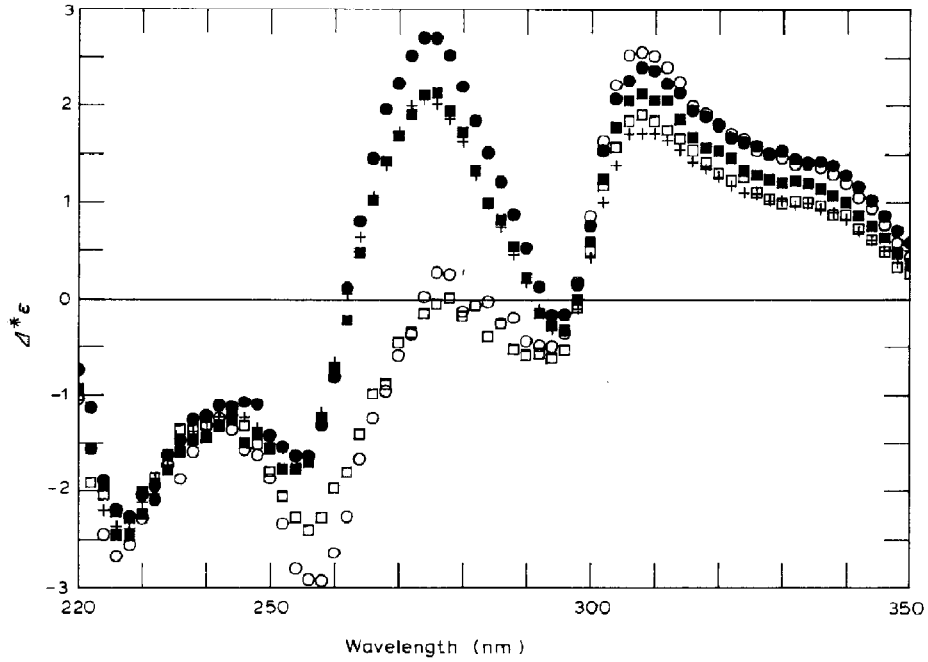

Fig. 2. CD $\Delta^*\epsilon$ (in $M^{-1}\,cm^{-1}$) spectra at various r values for native pEGF (□, native pACL29 (○), nicked pEGF (■), nicked pACL29 (●), and CT DNA (+). The r values were in the following order: 0.126, 0.135, 0.138, 0.147 and 0.125.

formation of the intercalation site vs r [21]. The latter suggestion is supported by CD measurements on dinucleotides intercalated with ethidium [21]. Furthermore, as can be seen from the plots in fig. 3, quadratic behavior begins at very low r values which correspond to the distances between intercalated molecules of ethidium being too large to support the proposed existence of exciton interactions.

Some complication arises from the strong absorption which is displayed at 280 nm by both DNA and ethidium, suggestive of a considerable degree of interaction which makes evaluation of the contribution by ethidium to the CD spectrum rather difficult. Two different contributions are expected for the 254 and 275 nm bands: an interaction between the dipoles of DNA bases and those of the ethidium in the particular geometrical configuration of the intercalation pocket (EB-base interaction) and another between neighboring DNA bases of different secondary structures in the intercalated B helix (base-base interaction). The location of both bands in the difference spectra is very close to that of the free DNA CD spectrum, thereby providing support for the proposed non-zero contribution by this base-base interaction. We attempted to determine the individual contribution by the base-base interaction to the CD spectra of both native and nicked forms of DNA by assuming the existence of the same geometry of the intercalation pocket in both supercoiled and nicked DNA, as discussed later.

The behavior of different forms of DNA plasmids can be summarized by plotting the differences in absolute values of the CD ($\Delta^*\epsilon$) maxima between supercoiled ($\Delta^*\epsilon_s$) and nicked ($\Delta^*\epsilon_n$) DNAs ($\Delta\Delta^*\epsilon = \Delta^*\epsilon_s - \Delta^*\epsilon_n$). The plots (fig. 4) appear to indicate differing extents of deformation of the nicked and supercoiled DNA structures due to intercalation. The major effect is observed in the 275 nm band (lowest curve), which shows essentially the same trend for both plasmids. The

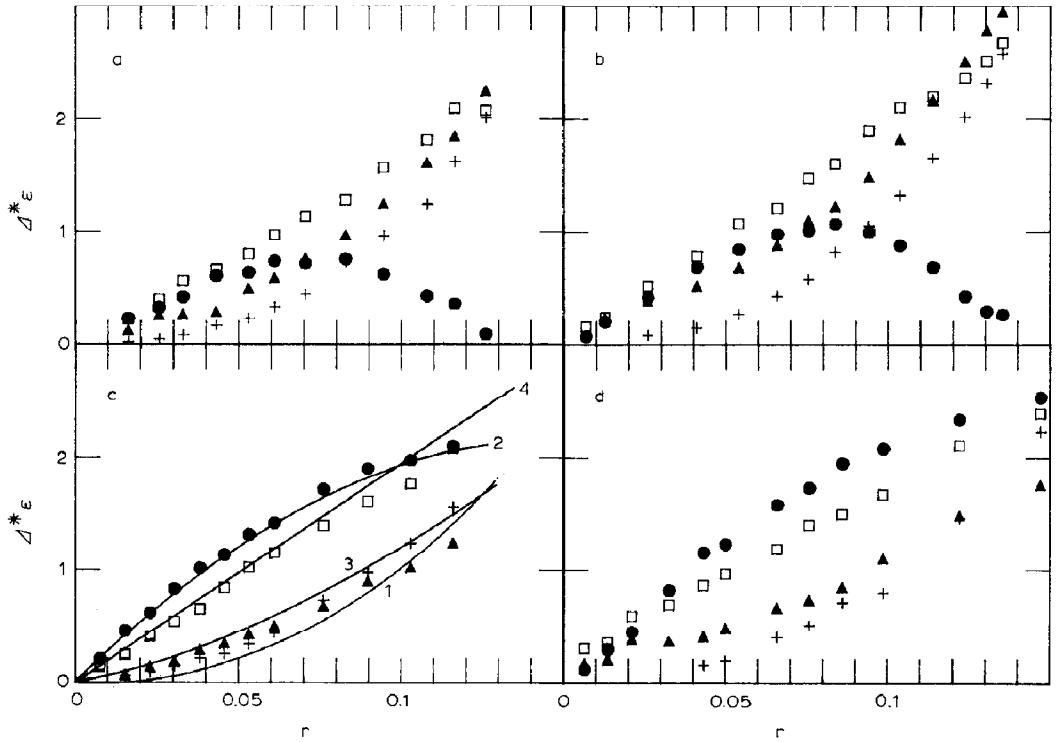

Fig. 3. Peak values of $\Delta^*\epsilon$ ($M^{-1}\,cm^{-1}$) spectra for (a) native pEGF, (b) native pACL29, (c) nicked pEGF, and (d) nicked pACL29. Symbols refer to different wavelengths: 308 nm (+), 275 nm (●), 254 nm (▲), 227 nm (□). Continuous lines 1–4 in panel c refer to data on calf thymus DNA at 308, 275, 254 and 227 nm, respectively.

other three bands plotted in fig. 4 show less pronounced effects that are only slightly larger than the errors.

Since supercoiled DNA undergoes dramatic changes in tertiary structure upon intercalation (superhelix detorsion, followed by relaxation and new torsion) when compared with the nicked form, differences in the secondary structure are also expected.

This is consistent with the data (fig. 4) which show deviation in linear behavior of $\Delta\Delta^*\epsilon$ at 275 and 254 nm with a sharp change in slope occurring at $r \cong 0.08$ for both plasmids. A linear trend in $\Delta\Delta^*\epsilon$ vs r could be attributed to the EB-induced alteration of some secondary structure parameter (e.g., twist or tilt angle), which grows with r, but in a different way for the native and the nicked forms of the plasmids.

Support for this proposed scheme, that excludes any contribution by EB-base interactions to the $\Delta\Delta^*\epsilon$ spectrum, is provided by the observation that a stronger dependence on r appears for the 254 and 275 nm bands, which are characteristic of the native DNA CD spectrum. In contrast, the 308 nm band, which can be assigned to the EB-base interaction, does not show any significant variation in the $\Delta\Delta^*\epsilon$ signal. It is therefore reasonable to assume that the geometry of the intercalation pocket is locally independent of the nicking. Otherwise, the 308 nm band would show more pronounced variation. The various changes in the native and nicked forms of plasmids might therefore be attributed to perturbations of the conformation of plasmids. The local deformation arising from the intercalation of ethidium may give rise, in the native DNA, to some strain extending well beyond the intercalation site. In contrast, for the nicked form, the strain induced by

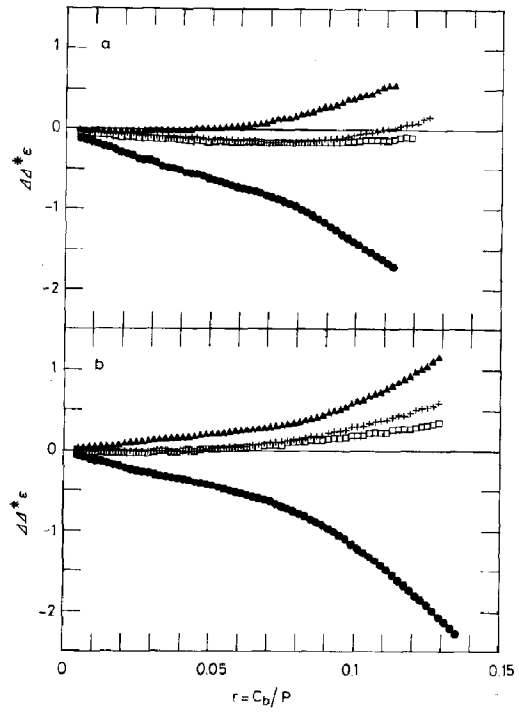

Fig. 4. Plots of $\Delta\Delta^*\epsilon$ ($M^{-1}\,cm^{-1}$) at different wavelengths for (a) pEGF and (b) pACL29. Symbols as defined in the legend to fig. 3.

ethidium should not extend much along the DNA chain, since strands are free to unwind. According to this description, the change in slope of the DNA bands (254 and 275 nm) occurring at $r \cong 0.08$ should then be taken as an indication of the different efficiency of ethidium in inducing deformations at low ($r \lesssim 0.08$) and high ($r \gtrsim 0.08$) intercalation ratios. Since the $\Delta\Delta^*\epsilon$ signal plotted in fig. 4 displays differences between supercoiled and nicked forms, which are known to be characterized by having distinct tertiary structures [1], this efficiency might be intrinsically linked to the tertiary structure of DNA.

4. DLS measurements

In order to test the above assumption, DLS investigation was performed. From low-angle measurements (25–30°) we determined the translational diffusion coefficient D_t of the plasmids at different values of r. The plot (fig. 5) of D_t vs r shows an initial range in which the behavior is roughly parabolic, followed by a region, beginning at $r = 0.08$, where a steep decrease occurs. Data in the latter interval of r were collected only for pEGF.

DLS measurements on pACL29 and pEGF in the native ($r = 0$) form were also carried out at different scattering angles ($30 < \theta < 130°$). From a double-exponential fit of the autocorrelation functions, two components were separated (D_t, D_2) [8,9]. The inverse of the slowest relaxation time $(\tau_1)^{-1}$ was found to be essentially linear with K^2 throughout the entire range of values of the scattering vector investigated ($0.5 \times 10^{10}\ cm^{-2} \leq K^2 \leq 6.15 \times 10^{10}\ cm^{-2}$), and resulted in a zero intercept at $K^2 = 0$: the gradient of this plot was taken as representing D_t, as is usually the case [8,9,22,23]. The second relaxation time τ_2 was plotted as the reciprocal vs K^2 in the form of $1/\tau_2$ as a function of $D_t K^2$. The intercept of the plot with the y-axis should be equal to $6D_r$ [22,23], where D_r denotes the rotational diffusion coefficient. The extrapolation of $1/\tau_2$ to $K^2 = 0$ is carried out by using a linear fit over the first few points ($K^2 \leq 1.5$–$2.0 \times 10^{10}\ cm^{-2}$), or a parabolic function over the whole range of K^2 investigated, with the added constraint that the linear term in K^2 is required to be equal to the experimental value of D_t as suggested recently [9,22]. The value of D_r and its variance, reported in table 1a, were computed using both estimates of the $1/\tau_2$ intercept at $K^2 = 0$.

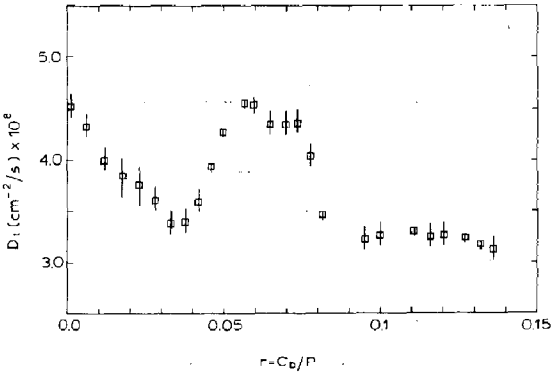

Fig. 5. Translational diffusion coefficient D_t for pEGF vs r.

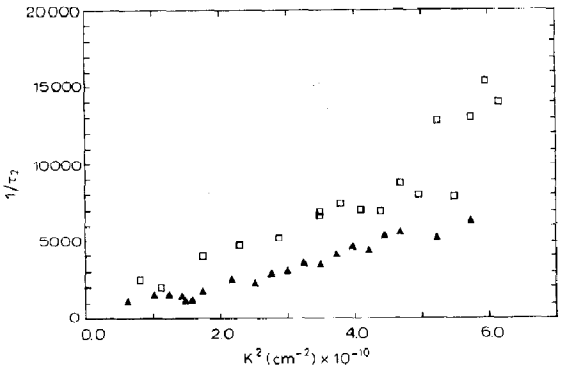

Fig. 6. Plot of the reciprocal of the faster relaxation time $1/\tau_2$ vs K^2 for native pEGF at $r = 0$ (□) and $r = 0.13$ (▲).

The same procedure was followed in the analysis of pEGF intercalated with ethidium at a ratio of $r = 0.13$, the values of D_t and D_r determined being listed in table 1a.

The initial range for D_t (fig. 5) vs r can be interpreted as being due to the ethidium-induced relaxation of supercoiled DNA. The unwinding of ethidium lowers β, the twist number, and since the linking number remains constant (eq. 5), the value of τ, the number of superhelical turns, increases and thereby gives rise to relaxation of the plasmid to a conformation which is much more open than that of the supercoil and, consequently, which has a lower value of the translational diffusion coefficient. On proceeding with the titration, the plasmid will undergo rewinding to the opposite handedness and D_t will increase again. A plot of D_t vs r should display a minimum, as indeed is found to be the case.

From eq. 5 and by using the value r_c corresponding to the minimum in D_t, the initial number of superhelical turns τ_0 can be estimated [9]. A more accurate estimate is obtained if the plasmid

Table 1

(a) Comparison between experimental data and theoretical predictions for the hydrodynamic parameters and (b) power laws [$D = AR^{-b}$ (toroidal) and $D = CH^{-d}$ (interwound)] describing the theoretically predicted values of D_t and D_r.

See text for further details. In part (a), the experimentally determined values of D_t are expressed in cm^2 s^{-1} × 10^{-8}, D_r in s^{-1}, H_0 in nm, R_0 in nm, and the computed values of D_t in cm^2 s^{-1} × 10^{-8} and of D_r in s^{-1}. In part (b), R and H are given in nm. D_t and D_r for pEGF at $r = 0$ and 0.13, and for pACL29 at $r = 0$ were computed for $\tau = -13.7$, 37 and −39, respectively.

(a)	D	D_{exp}	Toroidal		Interwound	
			R_0	$D(R_0)$	H_0	$D(H_0)$
pEGF ($r = 0$)	D_t	4.48 (±0.19)	110	3.65 $\chi^2 \cong 22$	372	4.60 $\chi^2 \cong 1.1$
	D_r	250 (±27)	110	300	372	240
pEGF ($r = 0.13$)	D_t	3.27 (±0.2)	174	2.95 $\chi^2 \cong 2.7$	620	4.00 $\chi^2 \cong 18$
	D_r	95 (±10)	174	100	620	81
pACL29 ($r = 0$)	D_t	3.24 (±0.1)	171	2.59 $\chi^2 \cong 57$	615	3.37 $\chi^2 \cong 2.3$
	D_r	72 (±5)	171	92	615	67.5
(b)	D		Toroidal		Interwound	
			A	b	C	d
pEGF ($r = 0$)	D_t [a]		57.31	0.586	66.846	0.446
	D_r [b]		0.339	1.98	2.89	2.277
pEGF ($r = 0.13$)	D_t [a]		64.34	0.598	150.3	0.56
	D_r [b]		15.75	2.77	57.28	2.45
pACL29 ($r = 0$)	D_t [a]		60.07	0.612	111.5	0.545
	D_r [b]		2.263	2.414	46.115	2.45

[a] A, C expressed in cm^2 s^{-1} × 10^{-8}.
[b] A, C expressed in s^{-1} × 10^7.

mass increment contribution due to EB intercalation is subtracted from D_t.

In fact, assuming no conformational change occurs in DNA, D_t should vary due to the mass increment resulting from ethidium intercalation. The correction $D_t^M(r)$ to the experimental values of D_t can be expressed as $D_t^M(r) = D_t^{exp}(0)(1 + 2r(M_{EB}/M_p))^{-b}$, where $D_t^{exp}(0)$ is the experimental value of D_t at $r = 0$, $M_{EB} \cong 394$ the molecular weight of ethidium, and $M_p \cong 350$ the mean molecular weight of a DNA base. We selected a value of $b = 0.55$ (± 0.05) for exponent b as suggested by data on D_t vs molecular weight for native plasmids [22]. The values of r_c and τ_0 were calculated to be $r_c = 0.044$ (± 0.004) and $\tau_0 = -39$ (± 2) for pACL29, and $r_c = 0.306$ (± 0.003) and $\tau_0 = -13.7$ (± 1.5) for pEGF. The values of r_c and τ_0 for the different plasmids, when estimated without considering the mass increment due to intercalation, are approx. 10% greater than those reported above. For $r \geq 0.11$ pEGF shows a sudden decrease in D_t down to $D_t = 3.6 \times 10^{-8}$ ($\pm 0.2 \times 10^{-8}$) cm^2/s.

5. Theoretical models: DLS

In order to clarify the reason for the abrupt decrease in D_t vs r, comparison of the experimentally determined D_t values with those computed for various superhelical static conformations should be useful. The estimates of D_t were based on De Haen's expression for the friction factor f of a polymer chain composed of N monomers [24]. Each monomer is simulated as a sphere of radius ρ and the polymer chain is pictured as a string of spheres ('bead model'). The expression, as given by De Haen [24], is as follows:

$$\left.\begin{aligned} f &= 6\pi\eta_0\rho N\left[1 + N^{-1}\sum_{i\neq j} p(x_{i,j})\right]^{-1} \\ p(x) &= x - \tfrac{7}{4}x^4 + \tfrac{9}{8}x^6 + \tfrac{13}{2}x^7 + \tfrac{8}{3}x^8 \\ &\quad + \tfrac{3}{4}x^9 - \tfrac{167}{6}x^{10} \end{aligned}\right\} \qquad (8)$$

where η_0 represents the viscosity of the solvent and $x_{ij} = \rho/R_{ij}$ denotes the sphere radius ρ divided by the distance R_{ij} between the i-th and j-th spheres.

Our estimate of D_t for long rods based on this formula is in good agreement ($\leq 1.5\%$) with the exact solution reported by De la Torre et al. [25]. When computing D_t for DNA, the molecule is pictured as a string of spheres with $\rho = 1.25$ nm which is equal to the reported hydrodynamic radius of the DNA B-helix [26–28]. Furthermore, we have computed D_t for several values of ρ and observed the variation to be less than 5%, corresponding to changes in ρ of up to 30% from $\rho = 1.25$ nm. A form suggested for DNA is that of a B-DNA helix wrapped as a curved helix around a torus [20]. This form has been previously suggested to occur on the basis of small-angle X-ray scattering studies on native plasmid solutions ($r = 0$) [29,30].

In contrast, electron microscopy [30] and DLS [8,9,22] measurements have thus far suggested an interwound form [20] for native DNA with the B-helix wound around a cylinder (of height H and diameter d). In order to discriminate between the two conformations, we have evaluated D_t for both the interwound and toroidal forms of plasmids pEGF and pACL29. In the interwound form, the independent geometrical parameters concerned are the pitch p of the superhelix and the number of superhelical turns τ, while in the toroidal form they are the large radius R of the torus and the number of superhelical turns τ. The superhelix diameter d and the toroidal small radius r are given by the constraint of fixed contour length [31].

The values of D_t obtained on varying the number of superhelical turns can be described to a very good approximation by power laws of the type $D_t = AR^{-b}$ and $D_t = CH^{-d}$ for the toroidal and interwound forms (table 1b), where A, b, C, and d are functions of both τ_0 and contour length. The values of $\tau_0 = -13.7$ for pEGF and $\tau_0 = -39$ for pACL29 correspond to the native form ($r = 0$), while $\tau = 37$ is determined for pEGF using eq. 5 at $r = 0.13$. In order to discriminate between the two conformations, additional data must be introduced and hence we chose the rotational diffusion coefficient (table 1a). It is possible to predict the behavior of D_r for a bead model with little computational effort, using the algorithm of Garcia De la Torre et al. [32]. This consists of an ap-

proximation of the formula of Garcia Bernal and Garcia De la Torre [33] for the rotational diffusional coefficient evaluated with the modified Oseen tensor [34] in order to take into account the effect of finite size of the spheres. This formula has proved rather accurate for rods, circles and several other simple shapes [32]. Also the D_r values for the toroidal and interwound conformations determined according to the bead model quoted above can be approximated by power laws (table 1b).

The values of H_0 (or R_0) which minimize the reduced χ^2:

$$\chi^2 = \sqrt{\left(\frac{D_t^{exp} - D_t(p)}{\sigma_{D_t}}\right)^2 + \left(\frac{D_r^{exp} - D_r(p)}{\sigma_{D_r}}\right)^2} \tag{9}$$

are listed in table 1a. In the preceding definition, $D_t^{exp}(\pm\sigma_{D_t})$, $D_r^{exp}(\pm\sigma_{D_r})$ and $D_t(p)$, $D_r(p)$ represent the experimental and theoretical values, respectively, of D_t and D_r, and p the structural parameter H (interwound) or R (toroid).

In the case of the native plasmid ($r = 0$), good agreement ($\chi^2 = 1.1$ for pEGF, and $\chi^2 = 2.3$ for pACL29; table 1a) is observed with the interwound form. On the other hand, when adopting the toroidal conformation very poor agreement occurs ($\chi^2 = 22$ for pEGF, and $\chi^2 = 57$ for pACL29; table 1a).

The resulting diameters of the interwound conformation are $d \cong 17$ and 10.9 nm, for pEGF and pACL29, respectively, which correspond to pitch angles for the superhelix of $\psi \cong 45$ and 43°, consistent with the predictions of Camerino-Otero and Felsenfeld [35].

For highly intercalated pEGF the situation is reversed and the agreement found between the experimental and computed values of D_t and D_r is better for the toroidal ($\chi^2 \cong 2.7$) than for the interwound conformation ($\chi^2 \cong 18$). These data therefore suggest that native ($r = 0$) plasmids in solution should be described by the interwound conformation.

From these simulations of the diffusional properties of DNA it is also possible to rationalize the entire behavior of D_t vs r for pEGF. With r increasing from r_0, the number of superhelical turns also increases from zero to almost 20 at $r = 0.08$. At this point, a discontinuity is observed in D_t. Branching of the interwound form to yield a cruciform or similar type of structure is unlikely, since the predicted D_t should be greater due to the more compact form. Furthermore, if the straight interwound form is retained, the height of the cylinder holding DNA at $r \cong 0.13$ should be approximately double compared to that at $r = 0$. However, from $r = 0.035$ onward, D_t is in fact observed to increase, thereby being in support of an interwound form of decreasing length. A trend toward abrupt inversion should be assumed if the interwound form is also retained at very high r. Such variation in D_t could also be characteristic of more drastic conformational changes in the tertiary structure.

According to the estimates of D_t and D_r (table 1a), it appears likely that a conformational transition, such as that from the interwound to the toroidal form, may account for this sudden decrease in D_t. However, at present, an accurate description of the role of electrostatic and elastic interactions leading to such a transition represents a difficult task.

Alternative explanations for the sudden decrease in D_t at high r values, such as aggregation or nicking of one of the DNA strands, can be discarded. In fact, static light scattering measurements at $\theta = 25°$ during titration with EB yield no evidence in favor of condensation or aggregation. Furthermore, since the CD signal $\Delta\Delta^*\epsilon$ increases at high r values, the possibility of nicking in native plasmids may be ruled out, otherwise a decrease of $\Delta\Delta^*\epsilon = \Delta^*\epsilon_s - \Delta^*\epsilon_n$ would be observed.

Finally, on recalling that the change in slope of $\Delta\Delta^*\epsilon$ occurs at the same r value where the second decrease in D_t begins, the results indicate yet again that, above $r \cong 0.08$, ethidium induces a conformational transition in DNA.

6. Conclusions

From combined CD and DLS measurements on pEGF and pACL29 plasmids, the following

conclusions on secondary and tertiary structure can be drawn.

(a) CD measurements on native and nicked plasmids suggest that EB intercalation induces changes in the secondary structure of DNA which differ between the native and nicked forms. The change in slope of the CD $\Delta\Delta^*\epsilon$ spectra vs r at $r \cong 0.08$ (fig. 4) is likely to indicate the response of closed DNA to the strains imposed on the molecule, which differ at low and high r.

(b) From a comparison of the experimentally determined D_t and D_r values with the computed hydrodynamic parameters, the interwound form appears to be more likely to occur in native DNA. The sudden change in D_t vs r observed at $r \cong 0.08$ may be considered as being due to the onset of a transition from the native interwound form to a toroidal conformation.

(c) The common changes occurring in the CD (fig. 4) and DLS (fig. 5) data when plotted vs r strongly suggest that differing tertiary structures are related to different ethidium-induced deformations of the secondary structure of closed DNA molecules.

Acknowledgments

We are indebted to Professor G. Badaracco (Dip. di Biologia, Università di Milano, Italy) for kindly providing the strain of the pEGF plasmid, assistance in his laboratory during purification and useful discussions. We are also grateful to Dr. J. Langowski (EMBL Outstation, ILL, Grenoble, France) for the gift of the pACL29 plasmid, collaboration at EMBL-ILL (Grenoble) on DNA extraction and helpful suggestions.

References

1 B. Alberts, D. Bray, J. Lewis, M. Raff, K. Roberts and J.D. Watson, Molecular biology of the cell, 2nd edn (Garland, New York, 1983).
2 S. Arnott, Biochem. Biophys. Res. Commun. 47 (1972) 1504.
3 K.B. Hall and M.F. Maestre, Biophysics 23 (1984) 2127.
4 W.C. Brunner and M.F. Maestre, Biophysics 13 (1974) 345.
5 M.K. Cowman and G.D. Fasman, Proc. Natl. Acad. Sci. U.S.A. 75 (1978) 4759.
6 M.F. Maestre and J.C. Wang, Biophysics 10 (1971) 1021.
7 A. Worcel and E. Burgi, J. Mol. Biol. 71 (1972) 127.
8 G. Chirico, P. Crisafulli and G. Baldini, Nuovo Cimento 11D(5) (1989) 745.
9 G. Chirico and G. Baldini, J. Mol. Liquids 41 (1989) 327.
10 W.D. Wilson and I.G. Lopp, Biophysics 18 (1979) 3025.
11 J.L. Bresloff and D.M. Crothers, J.Mol. Biol. 95 (1975) 103.
12 A. Davidson and B. Norden, Chem. Scr. 9 (1975) 49.
13 A. Davidson and B. Norden, Spectrochim. Acta 32A (1976) 717.
14 W.D. Wilson, C.R. Krishnamoorthy, Y. Wang and J.C. Smith Biophysics 24 (1985) 1941.
15 S. Aktipis and A. Kindelis, Biochemistry 12 (1973) 1213.
16 J.C. Wang, J. Mol. Biol. 89 (1974) 783.
17 T. Hsieh and J.C. Wang, Biochemistry 14 (1975) 527.
18 W. Bauer and J. Vinograd, J. Mol. Biol. 33 (1968) 141.
19 W. Bauer and J. Vinograd, J. Mol. Biol. 47 (1970) 419.
20 J.H. White and W.R. Bauer, J. Mol. Biol. 189 (1986) 329.
21 S. Dahl, A. Pardi and I. Tinoco, Jr, Biochemistry 21 (1982) 2730.
22 J. Langowski and U. Giesen, Biophys. Chem. 34 (1989) 9.
23 R. Pecora, J. Chem. Phys. 48 (1968) 4126.
24 C. de Haen, R.A. Easterly and D.C. Teller, Biophysics 22 (1983) 1133.
25 M.M. Tirado and J. Garcia de la Torre, J. Chem. Phys. 71 (1979) 2581.
26 H. Yamakawa and M. Fujii, Macromolecules 6 (1973) 407.
27 M.T. Record, C.P. Woodbury and R.B. Inman, Biophysics 14 (1975) 393.
28 P. Wu, B.S. Fujimoto and J.M. Schurr, Biophysics 26 (1987) 1463.
29 G.W. Brady, D.B. Fein, H. Lambertson, V. Grassain, D. Foos and C.J. Benham, Proc. Natl. Acad. Sci. U.S.A. 80 (1983) 741.
30 C.J. Benham, Biophysics 26 (1987) 9.
31 J. Newman, Biophysics 23 (1984) 1113.
32 J. Garcia de la Torre, M.C. Lopez Martinez and J.J. Garcia Molina, Macromolecules 20 (1987) 661.
33 J.M. Garcia Bernal and J. Garcia de la Torre, Biophysics 19 (1980) 751.
34 J. Garcia de la Torre and V.A. Bloomfield, Q. Rev. Biophys. 14 (1981) 81.
35 R.D. Camerino-Otero and G. Felsenfeld, Proc. Natl. Acad. Sci. U.S.A. 75 (1978) 1708.